Search for exotic spin-dependent couplings of the neutron with matter using spin-echo based neutron interferometry

S. R. Parnell, A. A. van Well, and J. Plomp
Faculty of Applied Sciences, Delft University of Technology, Mekelweg 15, 2629 JB Delft, Netherlands

R. M. Dalgliesh, N.-J. Steinke,* and J. F. K. Cooper
ISIS, Rutherford Appleton Laboratory, Chilton, Oxfordshire, OX11 0QX, United Kingdom

N. Geerits
Atominstitut, TU Wien, Stadionallee 2, 1020 Vienna, Austria

K. E. Steffen and W. M. Snow
Center for Exploration of Energy and Matter, Indiana University, Bloomington, Indiana 47408, USA

V. O. de Haan
BonPhysics Research and Investigations BV, Laan van Heemstede 38, 3297AJ Puttershoek, Netherlands

(Received 16 March 2020; accepted 14 May 2020; published 9 June 2020)

Various theories beyond the Standard Model predict new particles with masses in the sub-eV range with very weak couplings to ordinary matter which can possess spin-dependent couplings to electrons and nucleons. We report null results of a search for possible exotic spin-dependent couplings of the neutron which could be induced by the exchange of light weakly coupled bosons or spin-gravity coupling conducted using a spin-echo neutron spectrometer. We constrain the products g_A^2 and $g_A g_V$ of the axial vector coupling of the neutron to the matter of the Earth through the exchange of a weakly coupled vector boson for force ranges between the metre scale and the radius of the Earth. We also constrain the constants in some theories of exotic spin-gravity couplings.

DOI: 10.1103/PhysRevD.101.122002

I. INTRODUCTION

The question of whether or not the gravitational interaction can possess a component depending on the intrinsic spin of particles appears already at the level of classical general relativity (GR) and was also supported by the concept of quantum mechanical spin. It is a persistent theme in the theoretical literature on gravitation [1–3]. In GR, gravity is interpreted as spacetime curvature, and test-particle trajectories are geodesics. Spacetime torsion, a further natural geometric quantity that is available to characterize spacetime geometry, vanishes in GR. However, many models which extend GR include various types of nonvanishing torsion sourced by some form of spin density [4–6]. In such models, the coupling of torsion to spin is typically of the same strength as that of curvature to energy-momentum, and spin-density sources strong enough to generate measurable torsion effects are difficult to find or fabricate. One can take an alternative point of view and simply treat the question of the presence of torsion as an issue to be answered by experiment [7–14].

The possible existence of new interactions in nature with ranges of mesoscopic scale (millimeters to microns), corresponding to exchange boson masses in the 1 meV to 1 eV range and with very weak couplings to matter has been discussed for some time [1,15] and has recently begun to attract renewed scientific attention. Particles which might mediate such interactions are sometimes referred to generically as WISPs (weakly interacting sub-eV particles) [16] in recent theoretical literature. Many theories beyond the Standard Model, including string theories, possess extended symmetries which, when broken at a high energy scale, lead to weakly coupled light particles with relatively long-range interactions such as axions, arions, familons and Majorons [17–24].

A general classification of interactions between nonrelativistic fermions assuming only rotational invariance [25] reveals 16 operator structures involving the spins, momenta, interaction range and various possible couplings of the particles. Of these sixteen interactions, one is spin-independent, six involve the spin of one of the particles and the remaining nine involve both particle spins. Ten of

*Present address: Institut Laue-Langevin, 71 Avenue des Martyrs, CS 20156, 38042 Grenoble, Cedex 9, France.

these 16 possible interactions depend on the relative momenta of the particles. The addition of the spin degree of freedom opens up a large variety of possible new interactions to search for which might have escaped detection to date. Powerful astrophysical constraints on exotic spin-dependent couplings [26–28] exist from stellar energy-loss arguments, either alone or in combination with the very stringent laboratory limits on spin-independent interactions from gravitational experiments [29]. However, a chameleon mechanism could in principle invalidate some of these astrophysical bounds while having a negligible effect in cooler, less dense lab environments [30], and the astrophysical bounds do not apply to axial-vector interactions [25]. These potential loopholes in the astrophysical constraints, coupled with the intrinsic value of controlled laboratory experiments and the large range of theoretical ideas which can generate exotic spin-dependent interactions, has led to a growing experimental activity to search for such interactions in laboratory experiments.

Different experiments have sought for either a spin-dependent gravity effect or new spin-dependent interactions using macroscopic test masses [13], atomic magnetometers [31,32], hyperfine transitions in trapped ions [33], free fall experiments with atoms in different hyperfine states [34–36] including a Mach-Zehnder-type Raman atom interferometer [37] and atom interferometry [38]. In the analysis of the latter experiment a modified gravitational potential including a possible violation of the weak equivalence principle (WEP) and the presence of a spin-dependent gravitational mass was considered in the form $V_{g,A}(z) = (1 + \beta_a + kS_z)m_A gz$, where m_A is the rest mass of the atom, β_a is the anomalous acceleration generated by a nonzero difference between gravitational and inertial mass due to a coupling with a field with nonmetric interaction with gravity, k is a model-dependent spin-gravity coupling strength, and S_z is the projection of the spin along the gravity direction.

Spin and velocity-dependent interactions from spin-1 boson exchange can be generated by a light vector boson X_μ coupling to a fermion ψ with an interaction of the form $\mathcal{L}_I = \bar{\psi}(g_V\gamma^\mu + g_A\gamma^\mu\gamma_5)\psi X_\mu$, where g_V and g_A are the vector and axial couplings. In the nonrelativistic limit, this interaction gives rise to two interaction potentials of interest depending on both the spin and the relative momentum [39]: one proportional to $g_A^2\vec{\sigma}\cdot(\vec{v}\times\hat{r})$ and another proportional to $g_V g_A\vec{\sigma}\cdot\vec{v}$, where $\vec{\sigma}$ is the Pauli spin matrix.

Neutrons have been used for gravity measurements since the 1960's [40], and more recently they have been used with success to tightly constrain possible weakly coupled spin-dependent interactions of mesoscopic range [41]. A polarized beam of slow neutrons can have a long mean free path in matter and is a good choice for such an experimental search [42]. Piegsa and Pignol [43] reported improved constraints on the product of axial vector couplings g_A^2 in this interaction. Polarized slow neutrons which pass near the surface of a plane of unpolarised bulk material in the presence of such an interaction experience a phase shift which can be sought using Ramsey's well-known technique of separated oscillating fields [44]. These limits were improved in subsequent work using polarized slow neutron polarimetry [45]. Other experiments have constrained $g_V g_A^n$, where g_A^n is the axial vector coupling to the neutron. Yan and Snow reported constraints on $g_V g_A^n$ using data from a search for parity-odd neutron spin rotation in liquid helium [46]. Adelberger and Wagner [29] combined experimental constraints on g_V^2 from searches for violations of the equivalence principles and g_A^2 from other sources to set much stronger constraints on $g_V g_A^n$ for interactions with ranges beyond 1 cm. Yan [47] analyzed the dynamics of ensembles of polarized ^{3}He gas coupled to the Earth to constrain $g_V g_A^n$ for interactions with ranges beyond 1 cm with laboratory measurements.

The experiment described in this paper sought longer-range exotic spin-dependent interactions of the neutron which could be sourced by the Earth using a spin echo interferometry technique known as spin echo small angle neutron scattering (SESANS) [48–50]. A SESANS neutron spin echo spectrometer coherently splits and recombines the neutron paths of the interferometer using a series of shaped magnetic fields.

In the conventional horizontal configuration employed in almost all such instruments this spectrometer is not sensitive to such interactions because the two paths lie in the horizontal plane. However by rotating the instrument by 90 deg, such that one path through the interferometer is higher than the other, effects on the neutron wave function from the Earth may be observed. The spin-independent phase shift of the neutron from Newtonian gravity was observed in the famous Colella, Overhauser and Werner (COW) experiment using a perfect crystal interferometer [51]. The precision of the COW measurement on the neutron was improved by almost 1 order of magnitude using a neutron spin echo interferometer [52]. In that work it was shown that the gravitationally induced quantum phase shift of the neutron agreed to within 0.1% of the value expected from theory. This result resolved a long-standing discrepancy in the perfect crystal-based neutron COW measurements between theory and experiment at the 1% level [53–56]. However residual discrepancies in some aspects of the data were found. Since the two neutron paths which are coherently split and recombined in the SESANS spectrometer possess different spin states, this discrepancy raised the question of whether or not this residual difference could be due to an unexpected spin-dependent interaction of the neutron dependent on its height above the Earth's surface. This result triggered the experiment reported in this paper.

II. THEORY

The Hamiltonian which describes the interactions in our experiment is given by

$$H(\vec{r}) = H_B(\vec{r}) + H_G(\vec{r}) + H_F(\vec{r}) + H_V(\vec{r}) + H_A(\vec{r}). \quad (1)$$

The first term describes the interaction with the magnetic flux $\vec{B}(\vec{r})$ at location $\vec{r}$,

$$H_B(\vec{r}) = -S_B\vec{\sigma}\cdot\vec{B}(\vec{r}), \quad (2)$$

where the magnetic interaction energy is $S_B = 60.2$ neV/T. The second term describes the gravitational interaction between the neutron and all source particles,

$$H_G(\vec{r}) = \sum_i h_G(\vec{r}-\vec{s}_i), \quad (3)$$

where $\sum_i$ denotes the sum over all source particles at locations $\vec{s}_i$ (similar equations are used for H_F, H_V and H_A as they are also defined as interparticle interactions). Further,

$$h_G(\vec{r}) = -\frac{Gmm_i}{r}(1+\beta_a)e^{-\frac{r}{\lambda_c}}, \quad (4)$$

where G is the gravitational constant, m the mass of the neutron and m_i the masses of the source particles. β_a parametrizes a possible acceleration generated by a nonzero difference between gravitational and inertial mass [38,57] and λ_c is an interaction range. The third term is a spin-gravity coupling similar to the one used by [38]. For each source particle we have

$$h_F(\vec{r}) = -\frac{h^2}{2mr}\left(\frac{1}{\lambda_c}+\frac{1}{r}\right)e^{-\frac{r}{\lambda_c}}g_F\vec{\sigma}\cdot\frac{\vec{r}}{r}, \quad (5)$$

where h is the Planck constant and g_F is a spin-gravity coupling strength constant. The fourth term comes from single vector boson exchange [39,43] yielding for each source particle,

$$h_V(r) = \frac{\hbar^2}{m\lambda r}e^{-\frac{r}{\lambda_c}}g_V g_A\vec{\sigma}\cdot\frac{\vec{v}}{v}, \quad (6)$$

where $\hbar = h/2\pi$, λ equals the neutron wavelength, $\vec{v}$ the velocity of the neutron with respect to the source particle, g_V is the vector coupling and g_A is the axial vector coupling constant. Note that to measure H_V the neutron-polarization precession plane must be parallel to the neutron velocity. The fifth term also comes from single vector boson exchange [39,43] so that again for each source particle,

$$h_A(r) = \frac{\hbar^3}{8m^2c\lambda r}\left(\frac{1}{\lambda_c}+\frac{1}{r}\right)e^{-\frac{r}{\lambda_c}}g_A^2\vec{\sigma}\cdot\left(\frac{\vec{v}}{v}\times\frac{\vec{r}}{r}\right), \quad (7)$$

where c is the speed of light. To measure h_A the precession plane must be horizontal and perpendicular to the neutron velocity.

Assume that all nucleons in the Earth (with mass M and radius R) act as a source, then the second term of the Hamiltonian becomes

$$H_G(r) = -\eta(z,\lambda_c,R)S_G(1+\beta_a), \quad (8)$$

where $S_G = mgR = 0.615$ eV with g the gravitational acceleration and

$$\eta(z,\lambda_c,R) = \frac{e^{-\frac{z}{\lambda_c}}}{1+\frac{z}{R}}f\left(\frac{R}{\lambda_c}\right), \quad (9)$$

where z is the height above the Earth and

$$f(x) = \frac{3e^{-x}}{x^2}\left(\cosh x - \frac{\sinh x}{x}\right).$$

This function monotonically decreases from 1 for $x = 0$ via 0.41 for $x = 1$ and 0.014 for $x = 10$ to a limit of $3/(2x^2)$. When z changes, the distance to the source particles changes and hence also the coupling energy. When $z \ll R$ and $z \ll \lambda_c$ we have

$$\eta(z,\lambda_c,R) \approx \left(1-\frac{z}{R}\right)f\left(\frac{R}{\lambda_c}\right),$$

and this part of the Hamiltonian reduces to the standard one for the potential energy of a neutron in the Newtonian gravitational field of the Earth (i.e., $R \ll \lambda_c$),

$$H_G(r) = (z-R)mg(1+\beta_a). \quad (10)$$

The third term of the Hamiltonian becomes

$$H_F(r) = -\zeta(z,\lambda_c,R)S_F g_F\vec{\sigma}\cdot\vec{e}_z, \quad (11)$$

where $S_F = Mh^2/(m^2R^2) = 1.4\times10^{17}$ eV and

$$\zeta(z,\lambda_c,R) = \frac{1}{2}\left(\frac{R}{\lambda_c}+\frac{R}{R+z}\right)\frac{e^{-\frac{z}{\lambda_c}}}{1+\frac{z}{R}}f\left(\frac{R}{\lambda_c}\right). \quad (12)$$

When $z \ll R \ll \lambda_c$ we have

$$\zeta(z,\lambda_c,R) \approx 1-\frac{z}{R},$$

and this part of the Hamiltonian reduces to the one given by [38] if one uses $g_F = km^3R^3g/(Mh^2)$,

$$H_F(r) = mg(z-R)k\vec{\sigma}\cdot\vec{e}_z. \tag{13}$$

The fourth term of the Hamiltonian becomes

$$H_V(r) = \eta(z,\lambda_c,R)S_V(\lambda)g_V g_A\vec{\sigma}\cdot\frac{\vec{v}}{v}, \tag{14}$$

where $S_V(\lambda) = M\hbar^2/(m^2R\lambda)$. The sensitivity is inversely proportional to the neutron wavelength. For a wavelength of 0.18 nm it is 1.21×10^{32} eV. The fifth term of the Hamiltonian becomes

$$H_A(r) = \zeta(z,\lambda_c,R)S_A(\lambda)g_A^2\vec{\sigma}\cdot\left(\frac{\vec{v}}{v}\times\vec{e}_z\right), \tag{15}$$

where $S_A(\lambda) = M\hbar^3/(8m^3R^2c\lambda)$. Again, the sensitivity is inversely proportional to the neutron wavelength. For a wavelength of 0.18 nm it is 5.3×10^8 eV.

The terms for the axial coupling constants are inversely proportional to the neutron wavelength, and hence they can be discriminated by variation of the neutron wavelength from magnetic flux contributions to the Hamiltonian which are independent of the neutron wavelength as is obvious from the first term in the Hamiltonian. An addition of energy to the Hamiltonian will proportionally change the precession frequency of the polarization vector, according to

$$\Delta\omega = -\frac{2\pi}{h}H. \tag{16}$$

This induces a wavelength dependent shift of the spin-echo phase,

$$\Phi = \Delta\omega\frac{m\lambda L}{h}, \tag{17}$$

where L is the appropriate length along the neutron beam where the instrument is sensitive to the influence of the terms in H. In this case we will have a wavelength dependent shift for the magnetic field contribution of

$$\Phi_B = S_B\frac{2\pi m\lambda L_B B}{h^2}. \tag{18}$$

In the case of the gravitational couplings the contributions become

$$\Phi_G = -\delta\frac{2\pi m^2 g\lambda L_G}{h^2}(1+\beta_a), \tag{19}$$

and

$$\Phi_F = \delta\frac{2\pi m^2 g\lambda L_F}{h^2}k, \tag{20}$$

where L_G and L_F are the effective interaction distances. Note that, since the spatial separation δ of the two interferometer paths is proportional to the square of the neutron wavelength, the phase shifts Φ_G and Φ_F will actually be proportional to the cube of the wavelength and therefore experimentally distinguishable from the magnetic field phase shift Φ_B.

The terms from vector boson exchange are inversely proportional to the neutron wavelength, and hence they can be discriminated by variation of the neutron wavelength,

$$\Phi_V = \eta(z,\lambda_c,R)\lambda S_V(\lambda)\frac{2\pi mL_V}{h^2}g_V g_A, \tag{21}$$

and

$$\Phi_A = \zeta(z,\lambda_c,R)\lambda S_A(\lambda)\frac{2\pi mL_A}{h^2}g_A^2, \tag{22}$$

where L_V and L_A are the effective interaction distances.

III. EXPERIMENTAL DETAILS AND RESULTS

The experiment was conducted at the ISIS Pulsed Neutron and Muon Source using the Offspec instrument. Offspec is a time of flight instrument equipped with a series of four parallelogram shaped static magnetic fields each with an rf flipper at the center. The instrument has been described in a number of publications [58–60] and in our previous gravity experiment [52]. A schematic overview is presented in Fig. 1(b). In the first half of the instrument one separates the spin-up and spin-down eigenstates in space by a magnetic field, just to bring them back together in the second half of the instrument by a mirrored field configuration. In the vertical configuration the spin states will acquire different phases along the two paths due to the differences in gravitational potential and possibly due to the spin-dependent couplings of interest and the interference pattern will change accordingly. The splitting is achieved

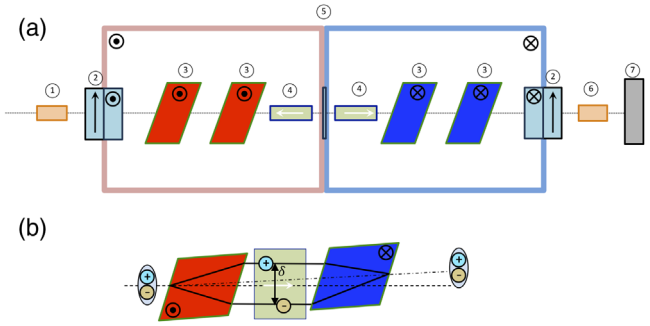

FIG. 1. Pictorial representation of the Offspec setup showing the beam line components and magnetic field orientations in (a), these are (1) polarizer, (2) v-coil ($\frac{\pi}{2}$ rotation), (3) rf flippers with shaped pole shoes, (4) Drabkin flipper with longitudinal magnetic field, (5) field stepper, (6) analyzer and (7) detector. In (b) is shown the operation of OffSpec (adapted from Ref. [52]).

by the gradient in the magnetic field across the beam [50]. The spin-echo phase is the difference between the phases acquired by the spin states along the two paths.

In the standard spin echo configuration of OffSpec the magnetic fields are perpendicular to the neutron beam and can be rotated to point in either the horizontal or vertical directions. This enables the measurement of the second term of the Hamiltonian (1). In the vertical direction, the gravitational potential energy of the upper spin state is larger than that of the lower spin state. Hence, the different H_G will yield different acquired phases, and they will not cancel each other, resulting in a finite spin-echo phase. The same holds for H_F and H_A as the sensitive directions are perpendicular to the beam.

To measure the H_V contributions we installed two Drabkin flippers [61] in the (otherwise empty) sample region of Offspec to put the neutron spin states into the direction longitudinal to the beam. These flippers consist of cylindrical magnetic-metal shields with end corrected solenoids and were operated in nonflip mode to adiabatically rotate and align the neutron spin along its longitudinal momentum vector and provide a longitudinal magnetic field parallel to the neutron trajectory. These flippers were placed on either side of the magnetic field stepper and are shown within the main guide field in Fig. 1(a). Both Drabkin flippers have a length of 400 mm, windings at a radius of 85 mm, and a magnetic-metal shield with radius 90 mm.

Similar to the procedure described in [52,59] the spin-echo-length constant was determined in both the vertical and horizontal modes. The result for the horizontal mode is shown in Fig. 2. The sample was a silicon grating with a calibrated period of 1.000 ± 0.001 μm. The scattering from the grating was analyzed using the phase object approximation [62]. The grating scattering length density

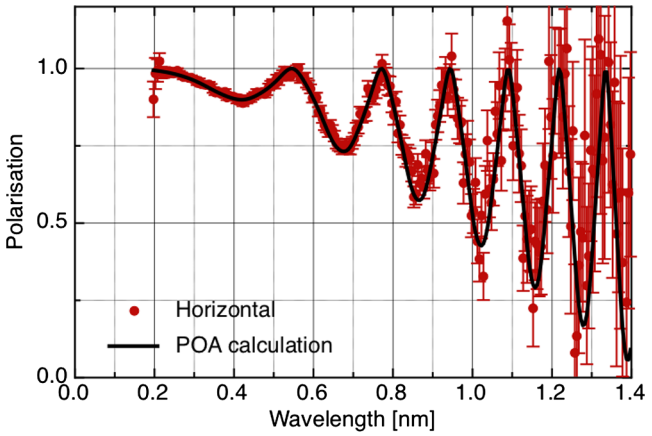

FIG. 2. Neutron polarization as a function of neutron wavelength analyzed by the neutron polarization analyzer at the exit of the interferometer in the horizontal mode as the coherently split neutron beam passes through the calibration grating. The solid line is a fit using the phase object approximation with a grating of 1 μm period.

profile was fitted to a trapezium shape with a height of 6.24 μm, a top width of 0.297 μm and a slope width of 0.123 μm. The wavelength scale of the instrument was calibrated with 1 part per thousand precision using a single crystal graphite crystal sample. The fitted spin-echo-length constant was 3.435(4) μm/nm^2 for the vertical case and 3.366(5) μm/nm^2 for the horizontal case.

As the same sample was used one might at first glance expect these values to be the same. The difference of 0.069(7) μm/nm^2, which is statistically significant, is probably due to the scattering of the neutron beam at the sample.

In [52] it was shown that the spin-echo condition is changed when the inclination angle of the neutron beam with respect to the horizontal is changed. In this case a tilt that generates 0.134 rad/nm^3/degree corresponds to a change in the spin-echo-length constant of 0.088 μm/nm^2. The scattering angle of the neutron beam at the sample is of the order of 1 deg; hence in the vertical mode the spin-echo condition changes due to a different path of the neutron beam through the second magnetic field region as a result of the scattering. This would change the measured polarization profile and hence the fitted spin-echo-length constant. In the horizontal mode the scattering angle does not influence the inclination angle of the beam, and hence the spin-echo condition remains unchanged. This combined effect of the tilt plus the scattering from the calibration sample could also explain the small systematic deviations in the results obtained previously in [52]. This is why we decided to use the horizontal results for the spin-echo-length constant only.

The measurements were done as in the previous experiment [52] and consisted of determining the polarization of the beam as a function of the spin-echo phase difference according to

$$P_m = P\cos\left(\Phi + (C_0 I_a + C_1)\lambda + C_2\lambda^2 + C_3\lambda^3\right), \qquad (23)$$

where Φ is the wavelength independent spin-echo shift and $C_0 = 2\pi m S_B (B_a/I_a) L_a/h^2$. I_a is the current through the second Drabkin coil which was scanned to be able to determine the phase, and B_a and L_a represent the active magnetic field and interaction distance for the phase shift contribution. C_1 represents the initial out-of-echo condition. We set C_2 to zero as this term is only influenced by the Sagnac effect, which is too small for us to resolve in this experiment [52]. $C_3 = (\Phi_G + \Phi_F)/\lambda^3$ is determined by the gravitational phase shift only. Note that C_3 is a constant independent of neutron wavelength or scan-coil current.

A scan consisted of varying the echo by adding an additional current I_a to the second Drabkin flipper (see Fig. 1). I_a was varied from $I_o - 0.5$ A to $I_o + 0.5$ A in 101 steps of 10 mA. The current I_o was chosen in such a way that the spin-echo was in balance position and varied between ± 0.5 A. An example of a data set is shown in

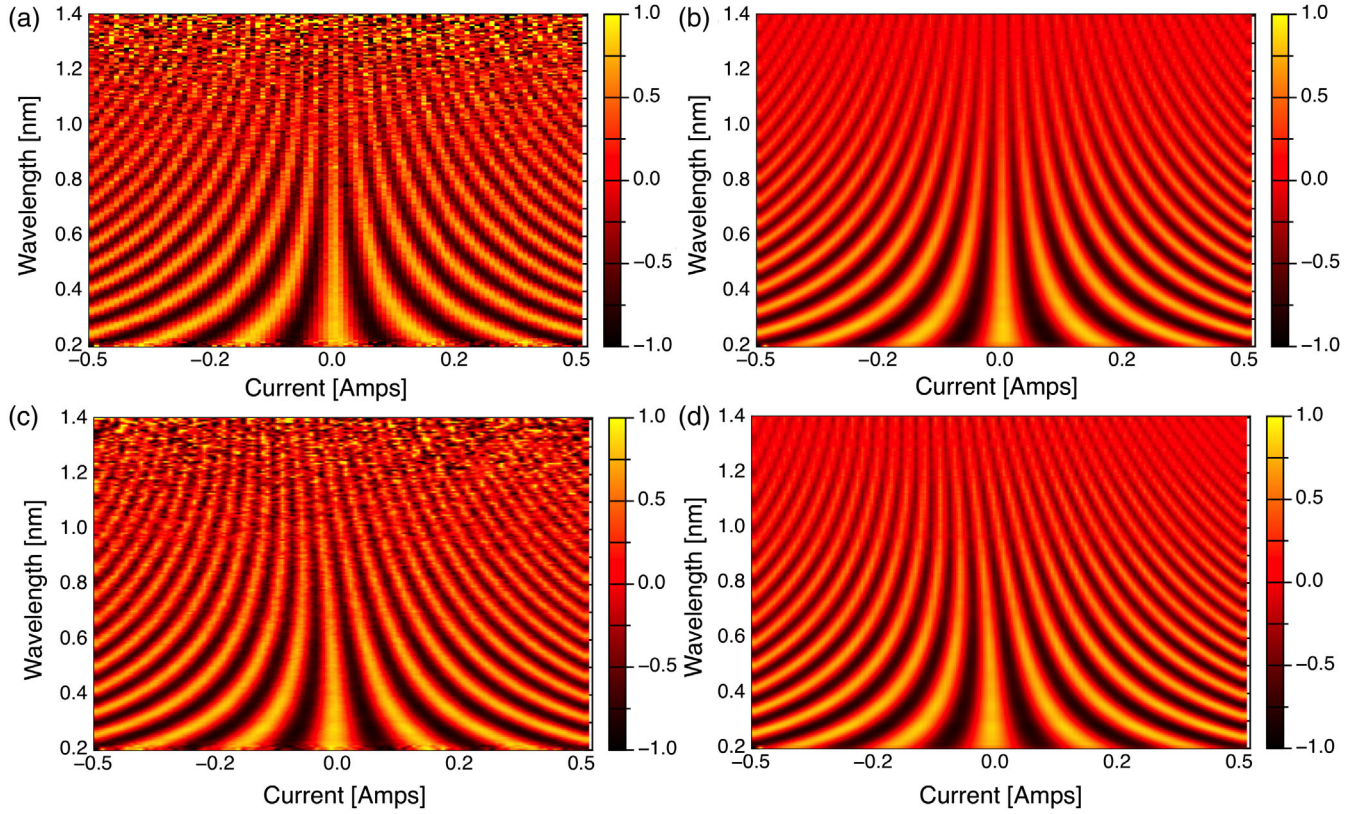

FIG. 3. Neutron polarization as a function of neutron wavelength and axial current for (a) horizontal mode and (b) the corresponding fit and (c) vertical mode and (d) the corresponding fit respectively.

Fig. 3 for both the horizontal (upper graphs) and vertical case (lower graphs). To the left the measurements are shown and to the right the corresponding fits. In the case with horizontal geometry the spin-echo condition does not depend on wavelength in contrast to the vertical mode. As the spin-dependent interaction of interest depends on the direction of the polarization vector with respect to the Earth and the beam direction, these data sets were measured in each mode for a total of 4 times differing by the parallel and antiparallel direction of the magnetic fields in each of the Drabkin coils. This enables the check of systematic effects in the determination of the fitted values. Additionally three different modes of OffSpec were used. One where the splitting occurred in the horizontal direction, one where the splitting occurred in the vertical direction and one where the splitting occurred in the vertical direction and the sign of the magnetic field regions was reversed. The results are shown in the Table I.

TABLE I. Fit results of constant and third order term. P denotes polarization vector parallel to the neutron beam and A denotes antiparallel. Estimated statistical standard deviations between brackets.

		Φ (rad)			C_3 (rad/nm^3)	
		P	A		P	A
Horizontal	P	0.094(3)	0.060(4)	P	−0.190(10)	−0.087(12)
	A	0.089(4)	0.028(5)	A	−0.110(13)	−0.058(15)
		P	A		P	A
Vertical I	P	0.077(4)	0.329(4)	P	5.158(11)	5.247(12)
	A	0.062(4)	0.253(3)	A	5.223(10)	5.237(10)
		P	A		P	A
Vertical II	P	0.244(4)	0.228(8)	P	5.207(11)	5.216(19)
	A	0.250(4)	0.222(8)	A	5.185(11)	5.176(20)

IV. DISCUSSION

The expected values when the coupling constants would be absent are 0 for Φ and -0.134 rad/nm^3 for C_3 in the horizontal mode and 5.239 rad/nm^3 for C_3 in the vertical modes. The value of C_3 is approximately a factor of 2 less than in the previous experiment [52]. This is due to different instrumental settings, in detail the magnetic field strength and the angle of the magnetic field regions with respect to the neutron beam.

The measured variation in the phase fit results with changing Drabkin coil current directions are in general very small. Less than 0.15 rad in case of the constant term and less than 0.08 rad/nm^3 for the third order term. This establishes a maximum value for the coupling constants.

TABLE II. Deviations of fit results with theoretical calculations of third order term taking all coupling constants set to 0. P denotes polarization vector parallel to the neutron beam and A denotes antiparallel. Estimated statistical standard deviations between brackets.

		ΔC_3 (rad/nm^3)	
		P	A
Horizontal	P	−0.056(10)	0.047(12)
	A	0.024(13)	0.076(15)
		P	A
Vertical I	P	0.083(11)	0.066(12)
	A	0.089(10)	0.060(10)
		P	A
Vertical II	P	−0.032(11)	−0.023(19)
	A	−0.054(11)	−0.063(20)

The β_a value of the Hamiltonian H_G contributes by changing C_3. In Table II the deviations from the theoretical values (with all coupling constants set to 0) in C_3 are shown. They are generally less than 0.1 rad/nm^3. This sets an upper limit on $f(\frac{R}{\lambda_c})\beta_a$ of 0.02. A similar value can be found for the contribution of Hamiltonian H_F, resulting in $k < 0.01$. This is a factor of 2 less than before because H_F is sensitive to the direction of the polarization. Hence, when the difference between two measurements, for which the effect is reversed, is used, the sensitivity doubles. Here we use the difference between vertical I and II. With respect to the limits established by [38] these values are quite poor, but this is the best limit to our knowledge for free neutrons. If k is translated to the coupling constant g_F this is limited to 4×10^{-20}.

The Hamiltonian H_V contributes only to the spin echo phase when the precession plane is perpendicular to the velocity of the neutron, hence inside the Drabkin coils. Depending on the direction of the current through the coils the phase is added or subtracted. Hence, the effective interaction length L_V is twice the path through both Drabkin coils as we compare the phase shifts when the effect in the coils is reversed hence 4×400 mm, $L_V = 1.6$ m and $\zeta g_V g_A < 0.11 \times 10^{-44}$. This bound is much lower than the neutron Ramsey method [43] and the Princeton results [63].

The contribution of the Hamiltonian H_A to the spin-echo phase is not reversed by the Drabkin coils. It reverses under the ±90 deg rotations from the horizontal position to the vertical configurations I and II. H_A influences the spin-echo phase inside the precession region but outside the Drabkin coils where the polarization vector and velocity vector are parallel. Hence the effective interaction range in this case is 2 times the distance traveled through the precession region minus the distance traveled through the Drabkin coils, $L_A = 2(3.85 - 0.80) = 6.1$ m and $\eta g_A^2 < 0.67 \times 10^{-22}$, so

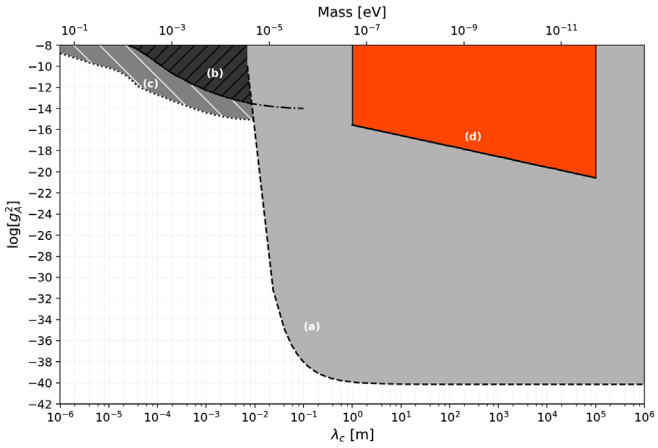

FIG. 4. Bounds on g_A^2 from several experiments. (a) refers to the Princeton K-He3 constraints [63] produced mathematically from the massless limit and formula specified in their paper, (b) refers to the Piegsa and Pignol copper constraint [43], (c) refers to the neutron spin rotation constraint [45] and (d) the new Offspec constraints are in red plotted from 1 m to 10^5 m for the apparatus height and Earth radius assumptions.

that when $\eta \approx 1$ then $g_A^2 < 0.67 \times 10^{-22}$. This bound is shown in Fig. 4. It is much lower than the neutron Ramsey method [43], but orders of magnitude higher than the Princeton results [63].

When the interaction distance is much less than the radius of the Earth, but longer than the height above Earth surface, then $\eta \approx 3\lambda_c^2/2R^2$ so that $g_V g_A < 0.27/\lambda_c^2 \times 10^{-31}$

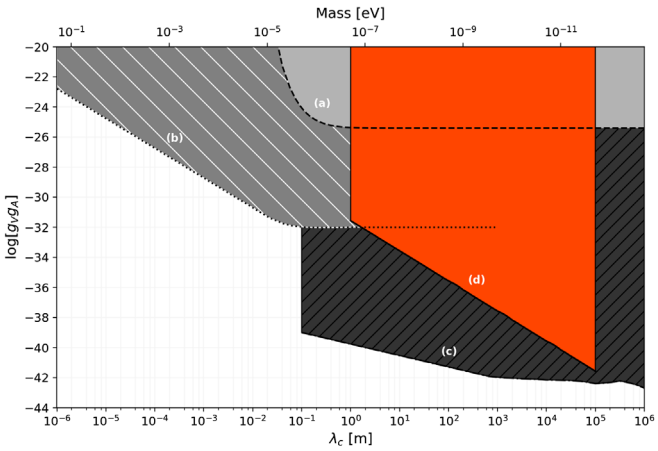

FIG. 5. Bounds on $g_V g_A$ from several experiments. (a) refers to the Princeton K-He3 constraints [63] produced mathematically from the massless limit and formula specified in their paper, (b) NSR n-^{4}He result which is a composite of the limits specified in the publication in order to approximately replicate the gradual drop off in sensitivity approaching 1 m. (c) is the approximate Adelberger composite constraint which was graphically sampled from the red dashed line of Fig. 1 in their publication [29] and (d) the new Offspec constraints are in red plotted from 1 m to 10^5 m for the apparatus height and Earth radius assumptions.

(λ_c in meters) which in this interaction range is much lower than both methods as shown in Fig. 5. In that case $\eta \approx 3\lambda_c/2R$ so that $g_A^2 < 0.27 \times 10^{-15}/\lambda_c$ (λ_c in meters) again in the interaction range much smaller than the neutron Ramsey method.

For the third order term the measurement noise has a 1.5% fractional error compared to the statistical error of about 0.4% (from 0.020 rad/nm^3). Hence, the statistical noise in the data is 3–4 times larger than expected from neutron counting statistics.

For the constant term the statistical accuracy estimated from neutron counting statistics is about 0.008 rad, which is also smaller than the observed noise. Table I shows that there are no obvious correlations between the values. The extra noise could be due to systematic variations from changes of several instrumental parameters which can influence the magnetic fields which are used to split and recombine the polarized neutron beam. These effects can include external magnetic field variations in the ISIS experimental hall, slow variations in the fields from the Drabkin coils, slow drifts in magnetic field parameters in components of the apparatus etc. Not all of the relevant magnetic fields in the apparatus which could produce such extra noise are monitored. In any future measurements which would attempt to improve these limits one would need to exercise more control over the magnetic field environment.

V. CONCLUSION

We have used a unique polarized neutron spin echo spectrometer Offspec at ISIS, which allows the plane of separation of the neutron paths in the interferometer to be shifted from the horizontal to the vertical plane, combined with the different direction of the neutron polarization states in each subbeam of this interferometer, to search for possible weakly coupled long range interactions from exotic vector boson exchange of the matter in the Earth that couple to the neutron spin. Our results are $\zeta g_V g_A < 0.11 \times 10^{-44}$ and $\eta g_A^2 < 0.67 \times 10^{-22}$. The precision of this measurement could be improved in principle with more extensive control of the magnetic field environment of the apparatus.

ACKNOWLEDGMENTS

The authors would like to thank *United Kingdom Science and Technology Facilities Council (STFC)* for the award of beam time for experiment RB1900118 and the data are available under [64]. We would also like to thank the referees for the positive comments. K. E. S. and W. M. S. acknowledge a grant for the US National Science Foundation Grant No. NSF-PHY 1913789 and the Indiana University Center for Spacetime Symmetries. N. Geerits acknowledges a grant from the Austrian science fund (FWF) Project No. P30677-N20.

[1] J. Leitner and S. Okubo, Phys. Rev. **136**, B1542 (1964).
[2] N. D. H. Dass, Phys. Rev. Lett. **36**, 393 (1976).
[3] T. S. K. Hayashi, Phys. Rev. D **19**, 3524 (1979).
[4] F. W. Hehl, P. von der Heyde, G. D. Kerlick, and J. M. Nester, Rev. Mod. Phys. **48**, 393 (1976).
[5] I. Shapiro, Phys. Rep. **357**, 113 (2002).
[6] R. Hammond, Rep. Prog. Phys. **65**, 599 (2002).
[7] S. Carroll and G. Field, Phys. Rev. D **50**, 3867 (1994).
[8] A. Belyaev, I. Shapiro, and M. do Vale, Phys. Rev. D **75**, 034014 (2007).
[9] B. R. Heckel, E. G. Adelberger, C. E. Cramer, T. S. Cook, S. Schlamminger, and U. Schmidt, Phys. Rev. D **78**, 092006 (2008).
[10] L. G. de Andrade, Mod. Phys. Lett. A **26**, 2863 (2011).
[11] C. Lämmerzahl, Phys. Lett. A **228**, 223 (1997).
[12] V. Kostelecký, N. Russell, and J. Tasson, Phys. Rev. Lett. **100**, 111102 (2008).
[13] W.-T. Ni, Rep. Prog. Phys. **73**, 056901 (2010).
[14] S. Capozziello and M. D. Laurentis, Phys. Rep. **509**, 167 (2011).
[15] C. Hill and G. G. Ross, Nucl. Phys. **B311**, 253 (1988).
[16] J. Jaeckel and A. Ringwald, Annu. Rev. Nucl. Part. Sci. **60**, 405 (2010).
[17] S. Weinberg, Phys. Rev. Lett. **29**, 1698 (1972).
[18] B. A. Dobrescu, Phys. Rev. Lett. **94**, 151802 (2005).
[19] T. Appelquist, B. A. Dobrescu, and A. Hopper, Phys. Rev. D **68**, 035012 (2003).
[20] A. Arvanitaki, S. Dimopoulos, S. Dubovsky, N. Kapoler, and J. March-Russell, Phys. Rev. D **81**, 123530 (2010).
[21] I. Bars and M. Visser, Phys. Rev. Lett. **57**, 25 (1986).
[22] S. M. Barr and R. N. Mohapatra, Phys. Rev. Lett. **57**, 3129 (1986).
[23] G. Lazarides, C. Panagiotakopoulos, and Q. Shafi, Phys. Rev. Lett. **56**, 432 (1986).
[24] K. A. Olive *et al.* (Particle Data Group), Chin. Phys. C **38**, 090001 (2014).
[25] B. A. Dobrescu and I. Mocioiu, J. High Energy Phys. 11 (2006) 005.
[26] G. Raffelt and A. Weiss, Phys. Rev. D **51**, 1495 (1995).
[27] G. Raffelt, *Stars as Laboratories for Fundamental Physics* (University of Chicago Press, Chicago, 1995).
[28] G. Raffelt, Phys. Rev. D **86**, 015001 (2012).
[29] E. G. Adelberger and T. A. Wagner, Phys. Rev. D **88**, 031101(R) (2013).
[30] P. Jain and S. Mandal, Int. J. Mod. Phys. D **15**, 2095 (2006).
[31] B. Venema, P. Majumder, S. Lamoreaux, B. Heckel, and E. Fortson, Phys. Rev. Lett. **68**, 135 (1992).
[32] D. F. J. Kimball, I. Lacey, J. Valdez, J. Swiatlowski, C. Rios, R. Peregrina-Ramirez, C. Montcrieffe, J. Kremer, J. Dudley, and C. Sanchez, Ann. Phys. (Amsterdam) **525**, 514 (2013).

[33] D. Wineland, J. Bollinger, D. Heinzen, W. Itano, and M. Raizen, Phys. Rev. Lett. **67**, 1735 (1991).
[34] S. Fray, C. A. Diez, T. W. Hansch, and M. Weitz, Phys. Rev. Lett. **93**, 240404 (2004).
[35] G. Rosi, G. D'Amico, L. Cacciapuoti, F. Sorrentino, M. Prevedelli, M. Zych, C. Brukner, and G. M. Tino, Nat. Commun. **8**, 15529 (2017).
[36] K. Zhang, M.-K. Zhou, Y. Cheng, L.-L. Chen, Q. Luo, W.-J. Xu, L.-S. Cao, X.-C. Duan, and Z.-K. Hu, arXiv: 1805.07758.
[37] X.-C. Duan, X.-B. Deng, M.-K. Zhou, K. Zhang, W.-J. Xu, F. Xiong, Y.-Y. Xu, C.-G. Shao, J. Luo, and Z.-K. Hu, Phys. Rev. Lett. **117**, 023001 (2016).
[38] M. G. Tarallo, T. Mazzoni, N. Poli, D. V. Sutyrin, X. Zhang, and G. M. Tino, Phys. Rev. Lett. **113**, 023005 (2014).
[39] F. M. Piegsa and G. Pignol, J. Phys. Conf. Ser. **340**, 012043 (2012).
[40] L. Koester, Z. Phys. **198**, 187 (1967).
[41] D. Dubbers and M. Schmidt, Rev. Mod. Phys. **83**, 1111 (2011).
[42] J. S. Nico and W. M. Snow, Annu. Rev. Nucl. Part. Sci. **55**, 27 (2005).
[43] F. M. Piegsa and G. Pignol, Phys. Rev. Lett. **108**, 181801 (2012).
[44] N. F. Ramsey, Phys. Rev. **78**, 695 (1950).
[45] C. Haddock *et al.*, Phys. Lett. B **783**, 227 (2018).
[46] H. Yan and W. M. Snow, Phys. Rev. Lett. **110**, 082003 (2013).
[47] H. Y. Yan, G. A. Sun, S. M. Peng, Y. Zhang, C. Fu, H. Guo, and B. Q. Liu, Phys. Rev. Lett. **115**, 182001 (2015).
[48] R. Gähler, R. Golub, K. Habicht, T. Keller, and J. Felber, Physica (Amsterdam) **229B**, 1 (1996).
[49] V. O. de Haan, *Coherence Approach to Neutron Propagation in Spin Echo Instruments*, 1st ed. (BonPhysics Research and Investigations B.V., The Netherlands, 2007).
[50] V. O. de Haan, A. A. van Well, and J. Plomp, Phys. Rev. B **77**, 104121 (2008).
[51] R. Colella, A. Overhauser, and S. Werner, Phys. Rev. Lett. **34**, 1472 (1975).
[52] V. O. de Haan, J. Plomp, A. A. van Well, M. T. Rekveldt, Y. H. Hasegawa, R. M. Dalgliesh, and N.-J. Steinke, Phys. Rev. A **89**, 063611 (2014).
[53] G. van der Zouw, M. Weber, J. Felber, R. Gahler, P. Geltenbort, and A. Zeilinger, Nucl. Instrum. Methods Phys. Res., Sect. A **440**, 568 (2000).
[54] K. C. Littrell, B. E. Allman, O. I. Motrunich, and S. A. Werner, Acta Crystallogr. Sect. A **54**, 563 (1998).
[55] J. Springer, M. Zawisky, R. Farthofer, H. Lemmel, M. Suda, and U. Kuetgens, Nucl. Instrum. Methods Phys. Res., Sect. A **615**, 307 (2010).
[56] B. Heacock, M. Arif, R. Haun, M. G. Huber, D. A. Pushin, and A. R. Young, Phys. Rev. A **95**, 013840 (2017).
[57] G. M. Tino, L. Cacciapuoti, S. Capozziello, G. Lambiase, and F. Sorrentino, Prog. Part. Nucl. Phys. **112**, 103772 (2020).
[58] J. Plomp, V. O. de Haan, R. M. Dalgliesh, S. Langridge, and A. A. van Well, Thin Solid Films **515**, 5732 (2007).
[59] J. Plomp, V. O. de Haan, R. M. Dalgliesh, S. Langridge, and A. A. van Well, Physica (Amsterdam) **406B**, 2354 (2011).
[60] S. R. Parnell, R. M. Dalgliesh, N. J. Steinke, J. Plomp, and A. A. van Well, J. Phys. Conf. Ser. **1021**, 012040 (2018).
[61] T. J. L. Jones and W. G. Williams, Nucl. Instrum. Methods **152**, 463 (1978).
[62] V. O. De Haan, J. Plomp, W. G. Bouwman, M. Trinker, M. T. Rekveldt, C. P. Duif, E. Jericha, H. Rauch, and A. A. van Well, J. Appl. Crystallogr. **40**, 151 (2007).
[63] G. Vasilakis, J. M. Brown, T. W. Kornack, and M. V. Romalis, Phys. Rev. Lett. **103**, 261801 (2009).
[64] V. O. de Haan, Measurement of spin-gravity coupling by quantum interference, STFC ISIS Facility, https://dx.doi.org/10.5286ISIS.E.RB1900118.